JOURNAL OF THERMOPHYSICS AND HEAT TRANSFER
Vol. 8, No. 3, July–Sept. 1994

Perturbation Analysis of Convective Heat Transfer in Helicoidal Pipes with Substantial Pitch

Y. Gong,* G. Yang,† and M. A. Ebadian‡
Florida International University, Miami, Florida 33199

Fully developed convective heat transfer in a coiled pipe with substantial pitch (the helicoidal pipe) is investigated by the perturbation method. The results of this study indicate that the effect of pitch on the temperature distribution appears in the second-order solution (T_2 terms), and that it will rotate the high temperature contours that deviate from the outer wall, which are enhanced by increasing the Reynolds number, the Prandtl number, and the curvature of the coil. As a result, the peak of the Nusselt number along the periphery moves away from the outer wall. The results of the study also indicate that increasing pitch may slightly reduce the average Nusselt number.

Nomenclature

B = pitch of the helicoidal pipe, m
D = diameter of the helix, m
De = Dean number
D_h = hydraulic diameter
Nu = Nusselt number
Pr = Prandtl number
p = pressure, N m^{-2}
Q = function, Eq. (6)
R = radius of the circular pipe, m
Re = Reynolds number
r = dimensionless radial direction coordinate
s = dimensionless axial coordinate
T = dimensionless fluid temperature
T_b = bulk temperature
T_w = wall temperature
u, v, w = dimensionless velocity components
$\bar{W}$ = dimensional reference velocity, m s^{-1}
α = thermal diffusivity, m^2 s^{-1}
β = function, Eq. (7)
γ = function, Eq. (8)
ε = dimensionless curvature, κR
η = function, Eq. (9)
θ = angular
κ = curvature, m^{-1}
λ = torsion
ν = kinematic viscosity, m^2 s^{-1}
ρ = density, kg m^{-3}
Φ = general variable
ω = function, Eq. (6)

Subscripts

c = curved pipe
$c2$ = the terms linked to cos 2θ
s = straight pipe
$s1$ = the terms linked to sin θ
0, 1, 2 = zero-, first-, and second-order solutions
20 = the terms linked to r only

Superscript

* = dimensional value

Received April 19, 1993; revision received Oct. 14, 1993; accepted for publication Oct. 20, 1993.

*Graduate Student, Department of Mechanical Engineering.
†Assistant Professor, Department of Mechanical Engineering.
‡Professor and Chairman, Department of Mechanical Engineering.

Introduction

COILED pipes, which in many cases have considerable pitch, are widely used in different engineering applications. The general subject of flow and heat transfer in coiled pipes has been examined by numerous researchers. Excellent surveys have been given by Berger et al.[1] and Shah and Joshi.[2] However, the majority of the studies conducted in the past have been based on the assumption of negligible pitch in the coiled pipe. Considering the effects of pitch will dramatically increase the complexity of the investigation since the pitch of the pipe will create an additional torsional force. In a toroidal pipe (referring to the coiled pipe with zero pitch in this article), two symmetrical loops of secondary flow are formed due to centrifugal force,[3] while in the helicoidal pipe (referring to the coiled pipe with a nonzero pitch), torsion will create a rotational motion that distorts the symmetrical loops of the secondary flow. Wang[4] obtained a first-order perturbation solution of the complete Navier-Stokes equation in a nonorthogonal helicoidal coordinate system. He presented his velocity field in contravariant components and found that torsion has a first-order effect on the secondary flow. Murata et al.[5] investigated laminar flow in a helicoidal pipe by both the perturbation and numerical methods. They presented their velocity field in covariant components and found that the torsion effect is of the second order. Germano[6] introduced a transformation to render the nonorthogonal coordinate system to an orthogonal one and found that the effect of torsion on the secondary flow is of the second order. Kao[7] used Germano's coordinate system to study flow in the helicoidal pipe in a substantial range of Dean numbers using both perturbation and numerical methods and concluded that the torsion effect may be on the order of one and a half. Recently, Tuttle[8] re-examined the same problem and pointed out that whether torsion has a first- or second-order effect on the secondary flow in a helicoidal pipe is really dependent on which frame of reference the observer used. However, compared with the study of flow in a helicoidal pipe, based on the authors' best knowledge, no paper has been published in the open literature to theoretically study the effect of pitch on convective heat transfer in a helicoidal pipe.

Fully developed convective heat transfer in a coiled pipe has been widely studied in the past century, and detailed reviews can be found in references by Baurmeister and Brauer,[9] and Shah and Joshi.[2] Interestingly enough, although the experimental results are usually obtained from the coiled pipe with a certain pitch, the majority of the numerical and theoretical solutions of convective heat transfer in a coiled pipe have focused on the case of a toroidal pipe where the torsion effect has been neglected. Recently, Yang et al.[10] studied

convective heat transfer in fully developed laminar flow in a nonzero pitch coiled pipe using a numerical method.

In this article, the perturbation method has been applied to solve fully developed convective heat transfer in a helicoidal pipe subjected to axially uniform wall heat flux with uniform peripheral wall temperature (H1). It is believed that the availability of such a solution can enrich our understanding of this important subject.

Governing Equations

Figure 1 shows the geometry of the helicoidal pipe and the coordinate system used in this study. In this figure, D and B represent the diameter and the pitch of the helix, respectively, and R is the radius of the circular pipe. s^*, r^*, and θ are the coordinates in the axial, radial, and tangential directions, respectively. If one uses u, v, and w to represent the radial, tangential, and axial velocities, and T for the fluid temperature, the dimensionless governing equations for fully developed laminar flow and convective heat transfer can be expressed as

$$\frac{1}{r}\frac{\partial u}{\partial \theta} + \frac{1}{r}\frac{\partial (rv)}{\partial r} + Q = 0 \tag{1}$$

$$\frac{u}{r}\frac{\partial u}{\partial \theta} + \frac{v}{r}\frac{\partial (ru)}{\partial r} = \frac{1}{Re}\left[-\frac{1}{r}\frac{\partial p}{\partial \theta} - \frac{u}{r^2} + \frac{1}{r}\frac{\partial u}{\partial r} + \frac{\partial^2 u}{\partial r^2} + \frac{1}{r^2}\frac{\partial v}{\partial \theta} - \frac{1}{r}\frac{\partial^2 v}{\partial r \partial \theta} - \varepsilon\omega\left(\eta\cos\theta - \lambda\frac{\partial \beta}{\partial \theta}\right)\right] + \varepsilon\omega\left(w^2\sin\theta + \lambda w\frac{\partial u}{\partial \theta}\right) \tag{2}$$

$$v\frac{\partial v}{\partial r} + \frac{u}{r}\frac{\partial v}{\partial \theta} = \frac{1}{Re}\left[-\frac{\partial p}{\partial r} + \frac{1}{r^2}\frac{\partial^2 v}{\partial \theta^2} - \frac{1}{r^2}\frac{\partial u}{\partial \theta} - \frac{1}{r}\frac{\partial^2 u}{\partial \theta \partial r} - \varepsilon\omega\left(\eta\sin\theta + \lambda\frac{\partial \gamma}{\partial \theta}\right)\right] + \frac{u^2}{r} - \varepsilon\omega w\left(w\cos\theta - \lambda\frac{\partial v}{\partial \theta}\right) \tag{3}$$

$$v\frac{\partial w}{\partial r} + \frac{u}{r}\frac{\partial w}{\partial \theta} = \frac{1}{Re}\left\{4\omega + \left(\frac{1}{r} - \varepsilon\omega\cos\theta\right)\frac{\partial w}{\partial r} + \frac{\partial^2 w}{\partial r^2} + \frac{\varepsilon\omega}{r}\sin\theta\frac{\partial w}{\partial \theta} + \frac{1}{r^2}\frac{\partial^2 w}{\partial \theta^2} - \varepsilon^2\omega^2 w - \varepsilon\lambda\left[\frac{1}{r}\frac{\partial}{\partial \theta}\left(\omega\frac{\partial u}{\partial \theta}\right) + \frac{\partial}{\partial r}\left(\omega\frac{\partial v}{\partial \theta}\right) + \frac{\omega}{r}\frac{\partial v}{\partial \theta}\right]\right\} - wQ \tag{4}$$

$$\frac{u}{r}\frac{\partial T}{\partial \theta} + v\frac{\partial T}{\partial r} = \frac{1}{PrRe}\left[\left(\frac{1}{r^2}\frac{\partial^2 T}{\partial \theta^2} + \frac{\partial^2 T}{\partial r^2} + \frac{1}{r}\frac{\partial T}{\partial r}\right) \times \varepsilon\omega\left(\frac{1}{r}\frac{\partial T}{\partial \theta}\sin\theta - \frac{\partial T}{\partial r}\cos\theta\right) + \varepsilon^2\omega^2\lambda^2\frac{\partial^2 T}{\partial \theta^2}\right] - \omega w + \varepsilon\omega\lambda w\frac{\partial T}{\partial \theta} \tag{5}$$

$$Q = \varepsilon\omega\left(u\sin\theta - v\cos\theta - \lambda\frac{\partial w}{\partial \theta}\right) \tag{6}$$

$$\beta = \frac{1}{r}\frac{\partial w}{\partial \theta} + \varepsilon\omega\left(w\sin\theta + \lambda\frac{\partial u}{\partial \theta}\right) \tag{7}$$

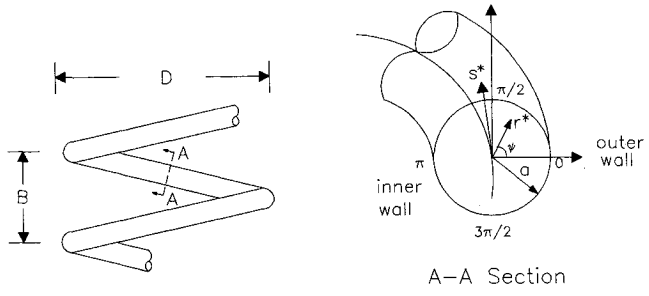

Fig. 1 Geometry and coordinate system of helicoidal pipe.

$$\gamma = \frac{\partial w}{\partial r} + \varepsilon\omega\left(w\cos\theta - \lambda\frac{\partial v}{\partial \theta}\right) \tag{8}$$

$$\eta = \frac{\partial u}{\partial r} + \frac{u}{r} - \frac{1}{r}\frac{\partial v}{\partial \theta} \tag{9}$$

The dimensionless parameters in Eqs. (1–5) are defined by

$$r = \frac{r^*}{R},\quad s = \frac{s^*}{R},\quad u = \frac{u^*}{W},\quad v = \frac{v^*}{W},\quad w = \frac{w^*}{\bar{W}}$$

$$p = \frac{p^*}{\rho\nu\bar{W}/R},\quad \varepsilon = \kappa R,\quad Re = \frac{\bar{W}\cdot R}{\nu},\quad Pr = \frac{\nu}{\alpha}$$

$$T = \frac{T^* - T_w^*}{\dfrac{4R_0^3\bar{W}^2}{\nu^2}\dfrac{dT_b^*}{ds^*}},\quad \bar{W} = \frac{R^2}{4\rho\nu}\left(-\frac{dp^*}{ds^*}\right) \tag{10}$$

$$\omega = \frac{1}{1 - \varepsilon\cos\theta},\quad \lambda = \frac{B}{\pi D},\quad De = Re^2\varepsilon$$

In Eq. (10), the value with a superscript * indicates the dimensional value, and

$$T_b^* = \frac{2}{\pi\bar{W}}\int_0^{\pi}\int_0^1 wT^* r\,dr\,d\theta \tag{11}$$

For fully developed flow with an axially uniform wall heat flux and a uniform peripheral wall temperature (H1) boundary condition, the boundary conditions for Eqs. (1–5) are

$$@\ r = 1$$
$$u = v = w = T = 0 \tag{12}$$
$$\frac{\partial p^*}{\partial s^*} = \text{const}$$
$$\frac{\partial T_b^*}{\partial s^*} = \text{const}$$

Equations (1–5) are derived based on Germano's coordinate system. There exists minor differences between Eqs. (1–4) of the present investigation and Germano's equations[6] due to the different definition of the dimensionless parameters and ω. The reason for using the current ω definition, which is different from Germano's, is to compare our velocity distribution with the results from Choi.[11] Equation (5), the energy equation, is derived in the helicoidal system by Yang et al.[10]

Perturbation Procedure and the Velocity Field

The perturbation technique has been used in this study to solve the governing equations, Eqs. (1–5). For the helicoidal pipe with a small curvature, it is natural to choose curvature

ε as the perturbation parameter. Therefore, unknown variables, u, v, w, p, and T, can be written in the general form:

$$\Phi = \Phi_0 + \varepsilon\Phi_1 + \varepsilon^2\Phi_2 + \cdots \tag{13}$$

In this study, only the first three terms will be considered. By substituting Eq. (13) into Eqs. (1–5) and collecting the terms with the same order of ε, one can obtain three sets of partial differential equations. Since the continuity and momentum equations are independent of the energy equation, the flowfield can be solved first.

The zero-order solution of the momentum equation represents Poiseuille flow in a straight pipe, which is

$$u_0 = v_0 = 0 \tag{14a}$$

$$w_0 = 1 - r^2 \tag{14b}$$

where the first- and second-order solutions represent the effects of curvature, which can be expressed as

$$u_1 = Re\left(-\frac{7r^6}{288} + \frac{5r^4}{48} - \frac{3r^2}{32} + \frac{1}{72}\right)\sin\theta \tag{15a}$$

$$v_1 = Re\left(\frac{r^6}{288} - \frac{r^4}{48} + \frac{r^2}{32} - \frac{1}{72}\right)\cos\theta \tag{15b}$$

$$w_1 = \left[\frac{3}{4}(-r^3 + r) + Re^2 \times \left(-\frac{r^9}{11520} + \frac{r^7}{1152} - \frac{r^5}{384} + \frac{r^3}{288} - \frac{19}{11520}r\right)\right]\cos\theta \tag{15c}$$

$$u_2 = \left[Re\left(-\frac{7r^7}{320} + \frac{r^5}{12} - \frac{71r^3}{810} + \frac{r}{80}\right) + Re^3\left(-\frac{r^{13}}{6635520} + \frac{r^{11}}{268800} - \frac{5r^9}{221184} + \frac{r^7}{12960} - \frac{481r^5}{3317760} + \frac{751r^3}{6967296} - \frac{14587r}{696729600}\right)\right]\sin(2\theta) + \lambda\left[\frac{r^4}{12} - \frac{r^2}{4} + 6 + Re^2\left(-\frac{17r^{10}}{69120} + \frac{47r^8}{23040} - \frac{13r^6}{2304} + \frac{49r^4}{6912} - \frac{79r^2}{23040} + \frac{13}{69120}\right)\right]\cos\theta \tag{16a}$$

$$v_2 = Re\left(\frac{r^7}{576} - \frac{r^5}{96} + \frac{r^3}{64} - \frac{r}{144}\right) + \left[Re\left(\frac{r^7}{240} - \frac{r^5}{48} + \frac{7r^3}{240} - \frac{r}{80}\right) + Re^3\left(\frac{r^{13}}{46448640} - \frac{r^{11}}{1612800} + \frac{r^9}{221184} - \frac{r^7}{51840} + \frac{481r^5}{9953280} - \frac{751r^3}{13934592} + \frac{14587r}{696729600}\right)\right]\cos(2\theta) + \lambda\left[\frac{r^4}{6} - \frac{r^2}{3} + \frac{1}{6} - Re^2\left(-\frac{r^{10}}{69120} + \frac{r^8}{7680} - \frac{r^6}{2304} + \frac{5r^4}{6912} - \frac{41r^2}{69120} + \frac{13}{69120}\right)\right]\sin\theta \tag{16b}$$

$$w_2 = \left(-\frac{11}{32}r^4 + \frac{7r^2}{16} - 3\right) + Re^2\left(-\frac{7r^{10}}{230400} + \frac{r^8}{3072} - \frac{r^6}{1152} + \frac{7r^4}{9216} + \frac{7r^2}{15360} - \frac{37}{57600}\right) + Re^4\left(-\frac{r^{16}}{106168320} + \frac{r^{14}}{5806080} - \frac{11r^{12}}{8847360} + \frac{157r^{10}}{33177600} - \frac{569r^8}{53084160} + \frac{11r^6}{737280} - \frac{331r^4}{26542080} + \frac{19r^2}{3317760} - \frac{1373}{1238630400}\right) + \left[\left(-\frac{15r^4}{16} + \frac{15r^2}{16}\right) + Re^2\left(-\frac{r^{10}}{6912} + \frac{7r^8}{5760} - \frac{101r^6}{30720} + \frac{269r^4}{69120} - \frac{463r^2}{276480}\right) + Re^4\left(-\frac{r^{16}}{731566080} + \frac{47r^{14}}{1857945600} - \frac{29r^{12}}{154828800} + \frac{61r^{10}}{79626240} - \frac{1241r^8}{597196800} + \frac{3881r^6}{1114767360} - \frac{1679r^4}{522547200} + \frac{883r^2}{731566080}\right)\right]\cos(2\theta) + \lambda\left[Re^3\left(\frac{r^{13}}{1451520} - \frac{7r^{11}}{691200} + \frac{r^9}{18432} - \frac{13r^7}{82944} + \frac{109r^5}{414720} - \frac{7r^3}{27648} + \frac{2969r}{29030400}\right) + Re\left(\frac{r^7}{192} - \frac{r^5}{72} - \frac{r^3}{24} + \frac{29r}{576}\right)\right]\sin\theta \tag{16c}$$

Equation (16) shows that torsion appears in the ε^2 terms in the u, v, and w velocity equations. Choi[14] also has expanded momentum equations to ε^3 terms. Therefore, Eqs. (15) and (16) in the present study have been compared with the first three terms (ε^0, ε^1, and ε^2) of Choi.[11] The results are almost identical after considering the difference in the definitions between the two studies.

Temperature Distribution

By substituting the velocities in Eqs. (14–16) into each order of the energy equations and solving these equations sequentially, one can obtain the zero-, first-, and second-order temperature distributions:

$$T_0 = \frac{Pr}{32Re}(r^4 - 4r^2 + 3) \tag{17a}$$

$$T_1 = \left[PrRe\left(-\frac{r^{11}}{2764800} + \frac{r^9}{184320} - \frac{r^7}{36864} + \frac{r^5}{13824} - \frac{19r^3}{184320} + \frac{73r}{1382400}\right) + Pr^2Re\left(-\frac{r^{11}}{552960} + \frac{r^9}{46080} - \frac{7r^7}{73728} + \frac{11r^5}{55296} - \frac{r^3}{4608} + \frac{103r}{1105920}\right) + \frac{Pr}{Re}\left(-\frac{r^5}{48} + \frac{5r^3}{64} - \frac{11r}{192}\right)\right]\cos\theta \tag{17b}$$

$$T_2 = \frac{Pr}{Re}\left(-\frac{5r^6}{768} + \frac{3r^4}{128} - \frac{5r^2}{192} + \frac{7}{768}\right)$$
$$+ PrRe\left(-\frac{r^{12}}{8294400} + \frac{7r^{10}}{3686400} - \frac{5r^8}{589824}\right.$$
$$\left. + \frac{11r^6}{663552} + \frac{r^4}{737280} - \frac{371r^2}{5529600} + \frac{2471}{44236800}\right)$$
$$+ Pr^2Re\left(-\frac{31r^{12}}{13271040} + \frac{101r^{10}}{3686400} - \frac{421r^8}{3538944}\right.$$
$$\left. + \frac{109r^6}{442368} - \frac{77r^4}{294912} + \frac{181r^2}{1474560} - \frac{3757}{265420800}\right)$$
$$+ PrRe^3\left(-\frac{r^{18}}{68797071360} + \frac{r^{16}}{2972712960}\right.$$
$$- \frac{11r^{14}}{3468165120} + \frac{157r^{12}}{9555148800} - \frac{569r^{10}}{10616832000}$$
$$+ \frac{11r^8}{94371840} - \frac{331r^6}{1911029760} + \frac{19r^4}{106168320}$$
$$\left. - \frac{1373r^2}{9909043200} + \frac{4741147}{84276412416000}\right)$$
$$+ Pr^2Re^3\left(-\frac{r^{18}}{57330892800} + \frac{7r^{16}}{16986931200}\right.$$
$$- \frac{29r^{14}}{7431782400} + \frac{263r^{12}}{12740198400} - \frac{37r^{10}}{530841600}$$
$$+ \frac{989r^8}{6370099200} - \frac{4241r^6}{19110297600} + \frac{409r^4}{2123366400}$$
$$\left. - \frac{73r^2}{796262400} + \frac{58721}{3210529996800}\right)$$
$$+ Pr^3Re^3\left(-\frac{r^{18}}{11466178560} + \frac{r^{16}}{566231040}\right.$$
$$- \frac{89r^{14}}{5945425920} + \frac{179r^{12}}{2548039680} - \frac{289r^{10}}{1415577600}$$
$$+ \frac{3943r^8}{10192158720} - \frac{1829r^6}{3822059520} + \frac{629r^4}{1698693120}$$
$$\left. - \frac{103r^2}{637009920} + \frac{97207}{3210529996800}\right)$$
$$+ \left[\frac{Pr}{Re}\left(-\frac{49r^6}{3072} + \frac{35r^4}{768} - \frac{91r^2}{3072}\right)\right.$$
$$+ PrRe\left(-\frac{41r^{12}}{77414400} + \frac{29r^{10}}{4423680} - \frac{53r^8}{1843200}\right.$$
$$\left. + \frac{289r^6}{4423680} - \frac{13r^4}{165888} + \frac{4153r^2}{116121600}\right)$$
$$+ Pr^2Re\left(-\frac{43r^{12}}{25804800} + \frac{151r^{10}}{8847360} - \frac{1447r^8}{22118400}\right.$$
$$\left. + \frac{271r^6}{2211840} - \frac{263r^4}{2211840} + \frac{14369r^2}{309657600}\right)$$
$$+ PrRe^3\left(-\frac{r^{18}}{468202291200} + \frac{47r^{16}}{936404582400}\right.$$
$$- \frac{29r^{14}}{59454259200} + \frac{61r^{12}}{22295347200} - \frac{1241r^{10}}{114661785600}$$
$$+ \frac{3881r^8}{133772083200} - \frac{1679r^6}{33443020800}$$
$$\left. + \frac{883r^4}{17557585920} - \frac{5137r^2}{249707888640}\right)$$
$$+ Pr^2Re^3\left(-\frac{29r^{18}}{3567255552000} + \frac{11r^{16}}{44590694400}\right.$$
$$- \frac{307r^{14}}{118908518400} + \frac{233r^{12}}{14863564800} - \frac{967r^{10}}{15288238080}$$
$$+ \frac{54377r^8}{334430208000} - \frac{9847r^6}{39636172800}$$
$$\left. + \frac{6989r^4}{33443020800} - \frac{783637r^2}{10701766656000}\right)$$
$$+ Pr^3Re^3\left(-\frac{r^{18}}{50960793600} + \frac{r^{16}}{2675441664}\right.$$
$$- \frac{r^{14}}{339738624} + \frac{61r^{12}}{4954521600} - \frac{299r^{10}}{10192158720}$$
$$+ \frac{497r^8}{12740198400} - \frac{131r^6}{5096079360}$$
$$\left. + \frac{11r^4}{2548039680} + \frac{533r^2}{267544166400}\right)\Bigg] \cos 2\theta$$
$$+ \lambda\left[Pr^3Re^2\left(\frac{r^{15}}{247726080} - \frac{13r^{13}}{185794560} + \frac{43r^{11}}{88473600}\right.\right.$$
$$- \frac{13r^9}{7077888} + \frac{23r^7}{5308416} - \frac{343r^5}{53084160} + \frac{103r^3}{17694720}$$
$$\left. - \frac{151r}{66355200}\right) + Pr^2Re^2\left(\frac{r^{15}}{206438400} - \frac{71r^{13}}{928072800}\right.$$
$$+ \frac{11r^{11}Re^4}{22118400} - \frac{11r^9}{5898240} + \frac{119r^7}{26542080} - \frac{151r^5}{22118400}$$
$$\left. + \frac{23r^3}{2686400} - \frac{163r}{66355200}\right) PrRe^2\left(\frac{r^{15}}{650280960}\right.$$
$$- \frac{r^{13}}{33177600} + \frac{r^{11}}{4423680} - \frac{13r^9}{13271040} + \frac{109r^7}{39813120}$$
$$\left. - \frac{7r^5}{1327104} + \frac{2969r^3}{464486400} - \frac{1199r}{390168576}\right)$$
$$+ Pr\left(\frac{r^9}{30720} - \frac{r^7}{6912} - \frac{r^5}{1152} + \frac{29r^3}{9216} - \frac{599r}{276480}\right)$$
$$\left. + Pr^2\left(-\frac{r^7}{6144} + \frac{r^5}{1536} - \frac{r^3}{1024} + \frac{r}{2048}\right)\right] \sin\theta \tag{17c}$$

Equation (17a) indicates that T_0, the temperature distribution in a straight pipe, is a function of r only. That is, the isothermal line will be a set of concentric circles, as seen in Fig. 2a. Equation (17b) indicates that T_1 is a function of both r and θ. However, since only the $\cos\theta$ term appears in Eq. (17b), T_1 is symmetric to the centerline, which is connected to the inner and outer walls, as seen in Fig. 2b. Figure 2b also shows that T_1 has a positive value in the semicircle near

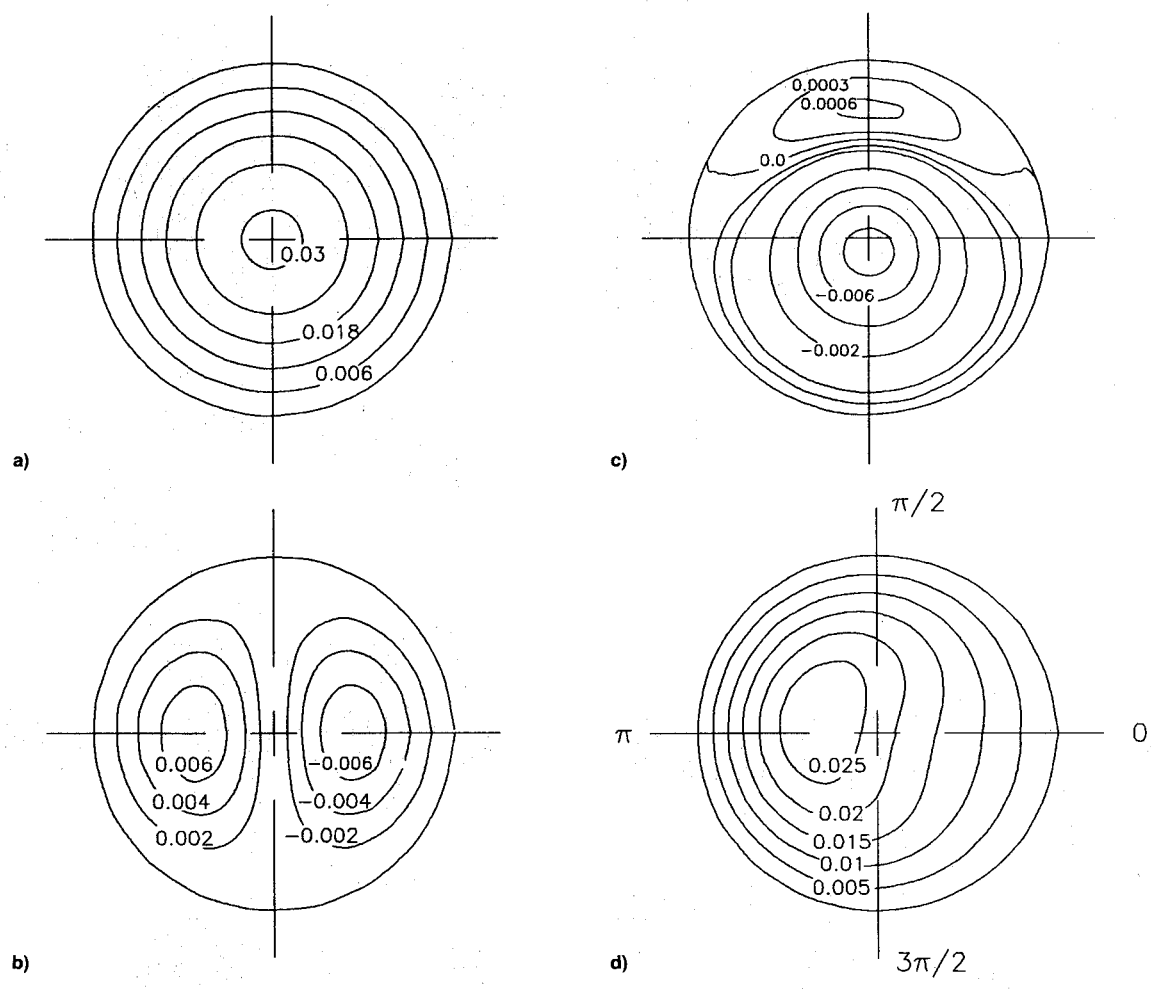

Fig. 2 Temperature distributions of T_0, T_1, T_2, and T: a) T_0, b) εT_1, c) $\varepsilon^2 T_2$, and d) $T = T_0 + \varepsilon T_1 + \varepsilon^2 T_2$.

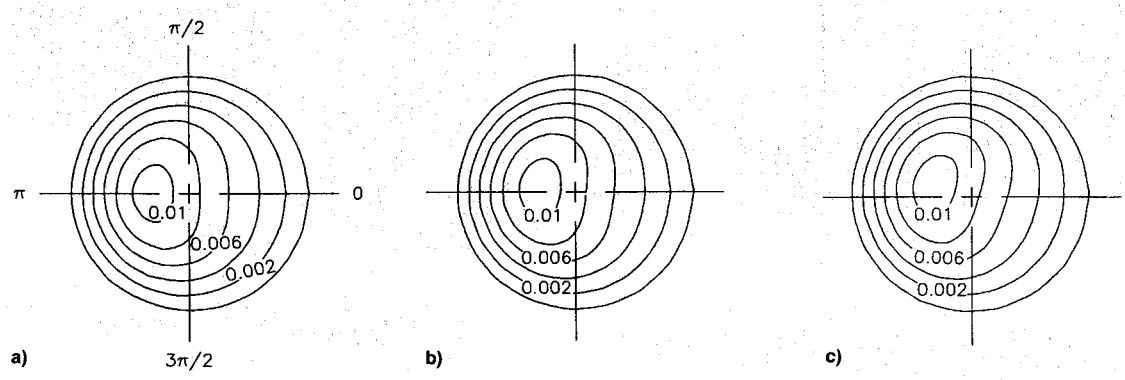

Fig. 3 Effect of torsion on the temperature distribution: a) $\lambda = 0.0$, b) $\lambda = 0.2$, and c) $\lambda = 0.5$.

the outer wall and a negative value near the inner wall. Equation (17c) shows that the second-order solution includes three parts: 1) the terms related to r only, T_{20}; 2) the terms related to both r and cos 2θ, T_{c2}; and 3) the terms related to r and sin θ, T_{s1}. The first two parts are symmetrical to the centerline between the innermost and outermost points or normal direction, while the third term is not. Generally speaking, T_{20} is the major term for heat transfer enhancement. Since the value of T_{c2} is almost two orders of magnitude less than that of T_{20}, the contributions of T_{c2} to the peripheral Nusselt number are trivial. The T_{s1} terms represent the contribution of torsion, which has the same order of magnitude as T_{20}. As expected, Fig. 2c shows that the contours of T_2 are highly asymmetrical with a negative value in the bottom region and a positive value in the top region. Equation (17) also indicates that the effect of pitch appears only in the T_2 solution and links to the asymmetrical terms of sin θ. If specifying that λ is equal to zero, Eq. (17) will reduce to a symmetrical solution, which corresponds to the case of a coiled pipe with a zero pitch. By combining the three parts, Fig. 2d shows the typical temperature distribution in a helicoidal pipe. The high temperature contours are not only pushed toward the outer wall, but are also rotated. During the calculation, parameters, $Pr = 10$, $Re = 30$, $\varepsilon = 0.1$, and $\lambda = 0.3$, have been applied.

Figure 3 illustrates the effect of torsion on the temperature contours, where parameters, $Re = 40$, $\varepsilon = 0.1$, and $Pr = 5.0$, have been used. When specifying $\lambda = 0$, Fig. 3a represents the temperature distributions in the toroidal pipe (zero pitch). Due to centrifugal force, the high temperature contours are pushed toward the outer wall. As the torsion increases to 0.2, Fig. 3b shows that the temperature contours rotate clockwise. Figure 3c shows that as the torsion further

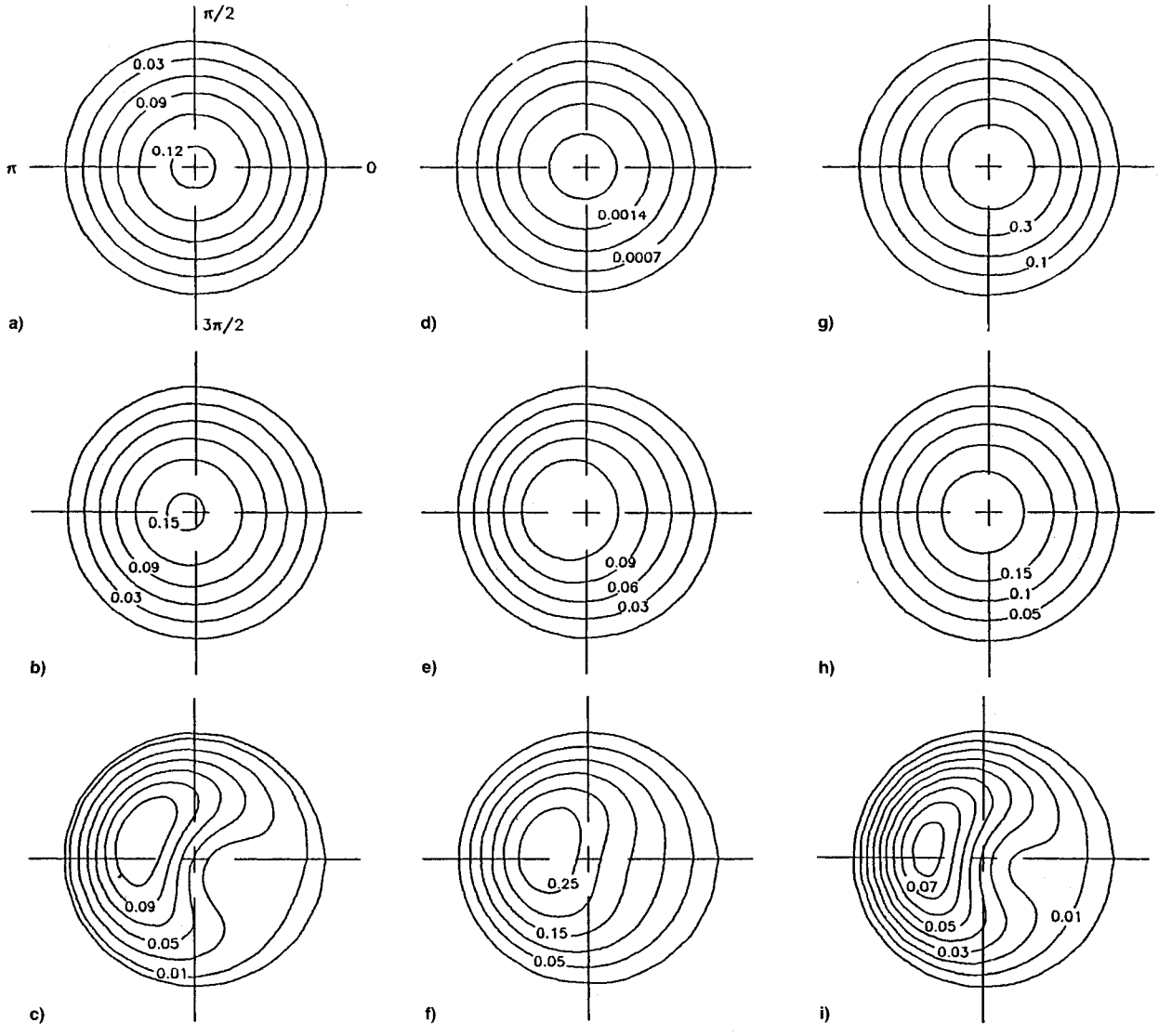

Fig. 4 Effect of torsion enhanced by other major parameters: a) $Pr = 5$, $Re = 30$, $\varepsilon = 0.01$, $\lambda = 0.3$; b) $Pr = 5$, $Re = 30$, $\varepsilon = 0.05$, $\lambda = 0.3$; c) $Pr = 5$, $Re = 30$, $\varepsilon = 0.3$, $\lambda = 0.3$; d) $Pr = 1$, $Re = 30$, $\varepsilon = 0.1$, $\lambda = 0.3$; e) $Pr = 5$, $Re = 30$, $\varepsilon = 0.1$, $\lambda = 0.3$; f) $Pr = 10$, $Re = 30$, $\varepsilon = 0.1$, $\lambda = 0.3$; g) $Pr = 5$, $Re = 1$, $\varepsilon = 0.1$, $\lambda = 0.3$; h) $Pr = 5$, $Re = 20$, $\varepsilon = 0.1$, $\lambda = 0.3$; and i) $Pr = 5$, $Re = 50$, $\varepsilon = 0.1$, $\lambda = 0.3$.

increases to 0.5, the angle of rotation increases. Figure 4 illustrates how other major parameters may enhance the effect of torsion. In these figures, the torsion has been fixed at 0.3. Figures 4a–4c indicate the effect of curvature on the temperature distributions, where $Pr = 5$, $Re = 30$, and ε changes from 0.01 to 0.3. As expected, there is no visible change in the temperature contours in the helicoidal pipe with a very small curvature (Fig. 4a, $\varepsilon = 0.01$). As ε increases to 0.05, Fig. 4b shows that the high temperature contours begin to move to the outer wall. However, it is still difficult to determine the contribution of torsion. In a helicoidal pipe with large curvature, the secondary flow becomes stronger and some of the temperature profiles appear as crescent shapes and the torsion rotates the contours. Figures 4d–4f represent the effect of the Prandtl number on the temperature distribution. The parameters, $Re = 30$ and $\varepsilon = 0.1$, are used in the calculation. The Prandtl number is the ratio of convective heat transfer over conductive heat transfer. Figure 4d shows that when $Pr = 1$, the appearance of the temperature contours remains as a concentric circle. As the Prandtl number increases to 5 (Fig. 4e), convective heat transfer becomes dominant and the temperature contours move toward the outer wall. However, the torsion effect still remains unimportant. When the Prandtl number is further increased, Fig. 4f shows that the temperature contours are significantly distorted and rotated. The Reynolds number is another important parameter to control heat transfer behavior in a helicoidal pipe. Figures 4g–4i show the effect of the Reynolds number on the temperature distribution, where parameters, $\varepsilon = 0.1$ and $Pr = 5$, are used. When Re is smaller than 20, Figs. 4g and 4h indicate that there is a very minimum torsion effect on the temperature contours. However, when Re reaches 50, a considerable distortion and rotation can be observed, as seen in Fig. 4i. Thus, Fig. 4 indicates that it appears that the torsion effect can be observed only when the temperature contours are significantly distorted.

Bulk Temperature

The bulk temperature is defined in Eq. (11), where the $\bar{W}$ can be found by

$$\bar{W} = \frac{\pi}{2} + \varepsilon^2 \left(\frac{-222125904\pi Re^4 - 383584481280\pi Re^2 + 12553673932800\pi}{1205152697548800} \right) \tag{18}$$

and the numerator can be written as

$$\int_0^{2\pi}\int_0^1 Twr\,dr\,d\theta = \sum_{i=0}^{2}\sum_{j=0}^{2}\int_0^{2\pi}\int_0^1 \varepsilon^{i+j}T_i w_j r\,dr\,d\theta \tag{19}$$

The nonzero terms in Eq. (19) are

$$\int_0^{2\pi}\int_0^1 T_0 w_0 r\,dr\,d\theta = \frac{11\pi Pr}{384Re} \tag{20a}$$

$$\int_0^{2\pi}\int_0^1 \varepsilon^2 T_0 w_2 r\,dr\,d\theta = \frac{\varepsilon^2(83290\pi PrRe^3 + 109034640\pi PrRe + 2107607040\pi Pr/Re)}{5885971660800} \tag{20b}$$

$$\int_0^{2\pi}\int_0^1 \varepsilon^2 T_1 w_1 r\,dr\,d\theta = \frac{\pi\varepsilon^2[(312583Pr^2 + 199504Pr)Re^3 + (-207662400Pr^2 - 395524800Pr)Re + 180104601600Pr/Re]}{117719433216000} \tag{20c}$$

$$\int_0^{2\pi}\int_0^1 \varepsilon^2 T_{20} w_0 r\,dr\,d\theta = -\frac{\varepsilon^2[(496795Pr^3 + 312583Pr^2 + 1665800Pr)Re^3 + (69220800Pr^2 + 2054131200Pr)Re + 217147392000Pr/Re]}{235438866432000} \tag{20d}$$

$$\int_0^{2\pi}\int_0^1 \varepsilon^4 T_{20} w_2 r\,dr\,d\theta = \varepsilon^4\left(\frac{6806898473\varepsilon^4 PrRe^7}{458929294020461356646400 0} + \frac{2402909055067\varepsilon^4 Pr^2Re^7}{261016035974137396592640 0000}\right.$$
$$+ \frac{103804160862113\varepsilon^4 PrRe^7}{274066837772844266422272000 00} - \frac{105363121\varepsilon^4 Pr^2Re^7}{329087029943992320000} + \frac{6324874273\varepsilon^4 PrRe^7}{1480891634747965440000} + \left.\frac{425273\varepsilon^4 PrRe^5}{753404372582400}\right) \tag{20e}$$

$$\int_0^{2\pi}\int_0^1 \varepsilon^4 T_{c2}\cos 2\theta w_2 r\,dr\,d\theta = \varepsilon^4\pi\left[-\frac{147612532591Pr^3Re^7}{730844900727584710459392 0000} + \frac{65994836288561Pr^2Re^7}{219253470218275413137817600000}\right.$$
$$+ \frac{5501480205989PrRe^7}{548133675545688532844544000 00} + \frac{3755209Pr^3Re^5}{118471330779837235200} - \frac{182030089357PrRe^5}{266560494254633779200000} - \frac{21679471943Pr^2Re^5}{621974486594145484800 00}$$
$$\left. - \frac{20201Pr^3Re^3}{602723498065920} + \frac{190918513Pr^2Re^3}{2373223773634560000} + \frac{262166473PrRe^3}{395537295605760000} - \frac{5423Pr^2Re}{15854469120} - \frac{673051PrRe}{1070176665600} + \frac{133Pr}{393216Re}\right] \tag{20f}$$

$$\int_0^{2}\int_0^1 \varepsilon^4 T_{c2}\sin\theta w_2 r\,dr\,d\theta = \lambda\varepsilon^4\pi\left[\left(\frac{1153699Pr^3Re^3}{403609485312000} + \frac{4375397Pr^2Re^3}{1412633198592000} - \frac{4241Pr^2Re}{5945425920} + \frac{6137PrRe}{1592524800}\right)\lambda\right.$$
$$\left. + \frac{113330407Pr^3Re^5}{32394504510111744000} + \frac{2455241813Pr^2Re^5}{647890090202234880000} + \frac{125257123PrRe^5}{23138931792936960000} - \frac{202091Pr^2Re^3}{235438866432000} + \frac{1366741PrRe^3}{151353556992000}\right] \tag{20g}$$

Equation (20) indicates that the torsion contribution to the bulk temperature is on the order of the ε^4 term, Eq. (20g).

Nusselt Number

The peripheral Nusselt number is defined as

$$Nu = \frac{2}{T_b}\left(\frac{\partial T}{\partial r}\right)_{r=1} \tag{21}$$

Substituting the T and T_b into Eq. (21), one can get

$$Nu = \frac{2}{T_b}\left\{\frac{Pr}{8Re} + \varepsilon\left(-\frac{29Pr^2Re}{552960} - \frac{11PrRe}{276480}\right.\right.$$
$$+ \frac{7Pr}{96Re}\cos\theta + \varepsilon^2\left[-\frac{1541PrRe^3}{33443020800} - \frac{29Pr^2Re}{1105920}\right.$$
$$- \frac{11PrRe}{138240} + \frac{Pr}{384Re} + \left(-\frac{281Pr^3Re^3}{133772083200}\right.$$
$$+ \frac{319Pr^2Re^3}{13934592000} + \frac{1261PrRe^3}{133772083200} - \frac{1577Pr^2Re}{77414400}$$
$$- \frac{1207PrRe}{58060800} + \frac{7Pr}{256Re}\cos 2\theta$$
$$+ \left(\frac{437Pr^3Re^2}{371589120} + \frac{79Pr^2Re^2}{61931520} + \frac{17PrRe^2}{7741440}\right.$$
$$\left.\left.\left.\left. - \frac{Pr^2}{3072} + \frac{17Pr}{7680}\right)\lambda\sin\theta\right]\right\} \tag{22}$$

Equation (22) indicates that the torsion contribution on the peripheral Nusselt number is through the $\sin\theta$ terms only. Figure 5 shows that the peripheral Nusselt number changes with torsion λ. $Re = 30$, $Pr = 10$, and $\varepsilon = 0.1$ have been applied during the calculation. The curve of $\lambda = 0$ indicates the case of a toroidal pipe that is symmetrical to the centerline. As λ increases, the peaks of the curve move to one side, which indicates an asymmetrical condition. Figure 5 also shows that the peak value of the peripheral Nusselt number slightly increases as λ increases. When $\lambda = 0.5$, this value increases by almost 5%.

By integrating Eq. (22) along the peripheral of the pipe

Table 1 Nu_c/Nu_s changes with torsion

	$\lambda = 0$	$\lambda = 0.1$	$\lambda = 0.3$
$Pr = 5$, $Re = 50$, $\varepsilon = 0.1$	1.0247	1.0240	1.0226
$Pr = 10$, $Re = 30$, $\varepsilon = 0.1$	1.0177	1.0176	1.0173
$Pr = 5$, $Re = 30$, $\varepsilon = 0.3$	1.0487	1.0457	1.0382
$Pr = 1$, $Re = 50$, $\varepsilon = 0.1$	1.0060	1.0059	1.0057

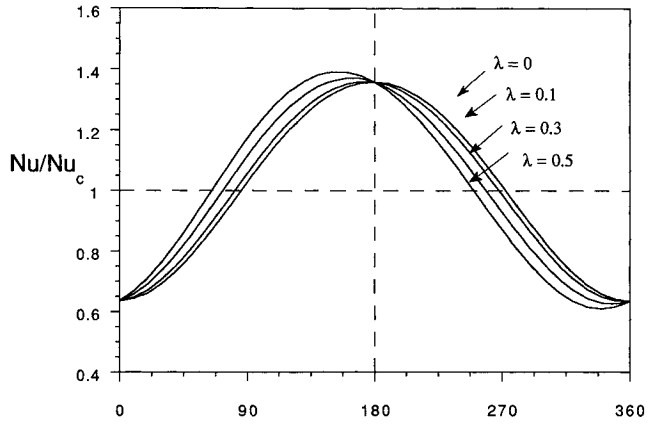

Fig. 5 Peripheral Nusselt number changes with torsion.

and averaging the results, one can obtain the average Nusselt number for the coiled pipe:

$$Nu_c = \frac{1}{2\pi}\int_0^{2\pi} \frac{2}{T_b}\left(\frac{\partial T}{\partial r}\right)_{r=1} d\theta$$

$$= \frac{2}{T_b}\left[\frac{Pr}{8Re} + \varepsilon^2\left(-\frac{1541PrRe^3}{33443020800} - \frac{29Pr^2Re}{1105920} - \frac{11PrRe}{138240} + \frac{Pr}{384Re}\right)\right] \quad (23)$$

Equation (23) indicates that the Nusselt number increase due to curvature is mainly contributed by the T_{20} terms. The contributions of other terms are only through the terms of T_b (Eqs. 20c, 20f, and 20g). Since the terms, T_1, T_{s1}, and T_{s2}, are trigonometric functions, integration along the periphery will be zero. This phenomenon can also be easily understood by looking at Fig. 2. For example, in Fig. 2b, the heat transfer enhancement of T_1 in the outer wall region will be counterbalanced by a reduction near the inner wall region.

Table 1 shows the effect of torsion on the Nusselt number in a helicoidal pipe. To emphasize the heat transfer enhancement, the Nusselt number ratio, Nu_c/Nu_s, has been used in this table, where $Nu_s = 4.3636$ represents the Nusselt number for straight pipe flow. The data indicate that the Nusselt number slightly decreases as torsion increases. For example, at $Pr = 5$, $Re = 30$, and $\varepsilon = 0.3$, the Nusselt numbers reduce about 0.29 and 1% when λ increases to 0.1 and 0.3, respectively. It needs to be emphasized that the validity range of this perturbation solution is limited by the momentum equations instead of the energy equation. Wang[5] indicated that $De = Re^2\varepsilon \leq 288$ can be used as a criterion for the flow solution. In this range of Dean numbers, Table 1 shows that only a slight increase of the Nusselt number can be achieved in a curved pipe, even if a significant change in the temperature profile can be reached.

Conclusions

Fully developed convective heat transfer in a coiled pipe with substantial pitch has been solved by the perturbation method. A closed-form solution of the temperature profile, periphery, Nusselt number, and the average Nusselt number has been found. The results indicate the following:

1) The effect of torsion on the temperature profile occurs only in the $\sin\theta$ terms in the second-order solution T_2. Torsion will rotate the temperature contours and destroy their symmetry.

2) The effect of torsion on the temperature distribution will be enhanced by increasing either the Reynolds number, the Prandtl number, or the curvature.

3) The effect of torsion on the peripheral Nusselt number is on the order of ε^2. Torsion will shift the peak of the Nusselt number deviating from the outer wall.

4) The effect of torsion on the average Nusselt number occurs only in the terms of T_b. As torsion increases, the Nusselt number will be reduced slightly. For example, at $Pr = 5$, $Re = 30$, and $\varepsilon = 0.3$, the Nusselt number will be reduced by 1% when torsion increases from zero to 0.3.

Acknowledgment

The results presented in this article were obtained in the course of research sponsored by the National Science Foundation (NSF) under Grant CTS-9017732.

References

[1]Berger, S. A., Talbot, L., and Yao, L. S., "Flow in Curved Pipes," *Annual Review of Fluid Mechanics*, Vol. 15, 1983, pp. 461–512.

[2]Shah, R. K., and Joshi, S. D., "Convective Heat Transfer in Curved Ducts," *Handbook of Single-Phase Convective Heat Transfer*, edited by S. Kakac, R. K. Shah, and W. Aung, Wiley Interscience, New York, 1987.

[3]Dean, W. R., "Note on the Motion of Fluid in a Curved Pipe," *Philosophical Magazine*, Vol. 4, 1927, pp. 208–223.

[4]Wang, C. Y., "On the Low-Reynolds Number Flow in a Helical Pipe," *Journal of Fluid Mechanics*, Vol. 108, 1981, pp. 185–194.

[5]Murata, S., Miyake, Y., Inaba, T., and Ogawa, H., "Laminar Flow in a Helically Coiled Pipe," *Bulletin of the Japan Society of Mechanical Engineers*, Vol. 24, 1981, pp. 355–362.

[6]Germano, M., "The Dean Equations Extended to a Helical Pipe Flow," *Journal of Fluid Mechanics*, Vol. 203, 1989, pp. 289–356.

[7]Kao, H. C., "Torsion Effect on Fully Developed Flow in a Helical Pipe," *Journal of Fluid Mechanics*, Vol. 184, 1987, pp. 335–356.

[8]Tuttle, E. R., "Laminar Flow in Twisted Pipes," *Journal of Fluid Mechanics*, Vol. 219, 1990, pp. 565–570.

[9]Baurmeister, U., and Brauer, H., "Laminar Flow and Heat Transfer in Helically and Spirally Coiled Tubes," *VDI Forschungsheft*, No. 593, 1979, pp. 2–48.

[10]Yang, G., Dong, Z. F., and Ebadian, M. A., "The Effect of Torsion on Convective Heat Transfer in a Helicoidal Pipe Heat Exchanger," 1992 ASME Winter Annual Meeting, General Papers in Heat Transfer, HTD 212, 1992, pp. 71–79, and ASME Transactions, *Journal of Heat Transfer*, Vol. 115, No. 3, 1993, pp. 796–800.

[11]Choi, S. W., "On Some Symptotics of Laminar Flow in a Coiled Pipe," Ph.D. Dissertation, Stanford Univ., Stanford, CA, 1987.